J. Synchrotron Rad. (1998). **5**, 998–1000

X-ray magnetic reflectometry using circularly polarized radiation

Claus Neumann,* Andrei Rogalev, José Goulon, Mik Lingham and Eric Ziegler

European Synchrotron Radiation Facility, BP 220, F-38043 Grenoble, France. E-mail: neumann@esrf.fr

(*Received 4 August 1997; accepted 10 November 1997*)

Magnetic reflectometry experiments have been performed in the X-ray range at the $L_{2,3}$ edges of rhodium. What makes these experiments original is the insertion of a very compact double-bounce reflectometer upstream of the monochromator. This configuration makes full use of the high polarization rate of the helical undulator source. This advantage is reflected in the high quality of the data obtained after only a few accumulations. It is also shown that, by properly selecting the angle of incidence, one may obtain experimental differential X-ray reflectivity spectra dominated either by the dispersion or the absorption terms.

Keywords: specular reflectivity; X-ray magnetic scattering.

1. Introduction

X-ray magnetic circular dichroism (XMCD) studies at the L or M absorption edges have become of much interest since it was realized that they allow the evaluation of the relative contributions of the orbital and spin moments at the absorbing centre in ferro(i)magnetic materials (Thole *et al.*, 1992; Carra *et al.*, 1993; Stöhr & Nakajima, 1997). Particularly exciting is the case of the (3*d*, *nd*) transition-metal alloys which exhibit giant magneto-resistances (Baibich *et al.*, 1988; Bisnasch *et al.*, 1989). Until recently (Harp *et al.*, 1995; Kobayashi *et al.*, 1996; Vogel *et al.*, 1997), experimental difficulties hampered XMCD studies at the $L_{2,3}$ edges of 4*d* elements: in the energy range of interest (*i.e.* 2.4–3.5 keV), the exit beam of an Si or Ge (111) double-crystal monochromator has a poor circular polarization rate since the Bragg angle approaches 45° (Malgrange *et al.*, 1991). In the present paper, we propose a strategy that consists of inserting the sample before the monochromator in order to take full benefit of the high circular polarization rate of the source. At low energy, transmission experiments are, however, to be avoided since ultra-thin samples are difficult to prepare and would not survive very long in a very intense undulator beam because of their very poor heat transfer. On the other hand, with a sample excited with a polychromatic beam, it does not make sense to measure the total electron yield (TEY) or the X-ray fluorescence yield (FY). We found it more attractive to perform differential X-ray reflectometry on what we call hereafter 'magnetic mirrors'. Our interest in this option was stimulated by recent reports by Kao *et al.* (1994) and Lambrecht *et al.* (1997) who observed large differences in the reflectivity of circularly polarized soft X-rays on flipping the orientation of the magnetization. The major differences between the former experiments and our own experiments are the following: (i) we do not use a monochromatic beam; (ii) we do not perform our experiments in the soft X-ray range but at photon energies greater than 2.4 keV. The present paper reviews all instrumentation problems associated with our specific experimental configuration. We will illustrate the performance of the technique with test experiments carried out at the $L_{2,3}$ edges of rhodium using a 'magnetic mirror' consisting of a silicon wafer coated with a thin film of $Fe_{67}Rh_{33}$ magnetic alloy.

2. Experimental

2.1. *Beamline configuration*

The reflectivity experiments described below were carried out at ESRF beamline ID12A, which is a windowless fully UHV beamline. A detailed layout of the beamline has been reported elsewhere (Goulon *et al.*, 1996, 1998). The helical undulator Helios-II (Elleaume, 1994) is well suited for investigations of the L edges of 4*d* transition metals: at low energies ($2.4 < E < 3.5$ keV), the undulator can be tuned at the first harmonic, which is quite intense and exhibits circular polarization rates in excess of 97% (Goulon *et al.*, 1996). The double-bounce reflectometer was installed in the 'white beam experimental station' (see Fig. 1 in Goulon *et al.*, 1998). The incident beam was collimated using water-cooled secondary slits located before the reflectometer and closed down to 400 (V) × 250 (H) μm. Indeed, the beam had to be strongly collimated horizontally because (i) the reflectometer deflects the beam in the horizontal plane; (ii) its angular acceptance is limited by the short lengths of the magnetic mirrors, which do not exceed 20 mm. We did not make use of a four-mirror (4-M) device even though it would have been preferable to pre-filter the high-energy radiation in order to minimize the heat load on the magnetic mirrors. The monochromator was equipped with a pair of Si (111) crystals cooled to 133 K and diffracting the X-ray beam in the vertical plane. Neither the 4-M

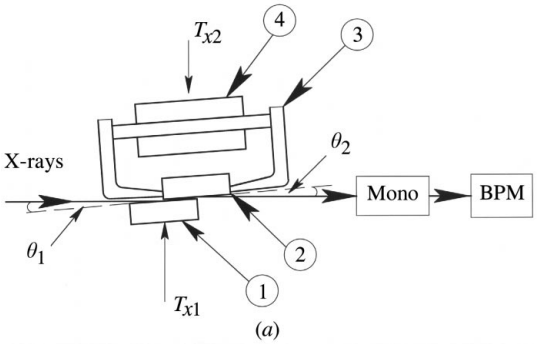

(*a*)

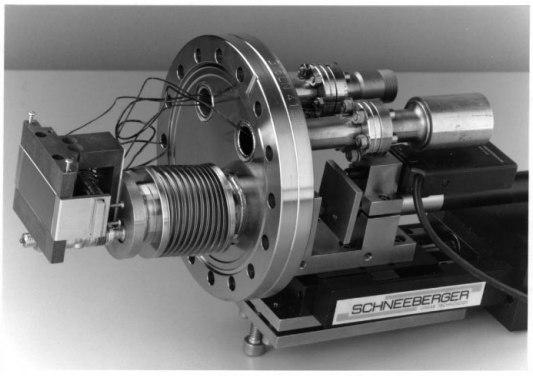

(*b*)

Figure 1
(*a*) Schematic layout (top view) of the double-bounce reflectometer. Mirror M_2 is coated with an active magnetic layer encompassed in a soft-iron magnetic circuit (3) magnetized by a coil (4). Mirror M_1 is not magnetic but is used to minimize the heat load and filter out harmonics. (*b*) Photograph of the entire mechanics.

device nor the magnetic reflectometer, which both deflect the beam in the horizontal plane, can spoil the measured energy resolution of the monochromator (0.44 eV), which is very close to the theoretical limit. The contamination of the spectra with high orders is already very low since the reflectometer plays the role of an extremely efficient harmonic filter because our measurements are performed very close to the critical angle of incidence. A multianode photodiode currently used as beam position monitor (BPM-2) was used as detector. Its spatial resolution is ±5 μm. By monitoring the beam displacement in the horizontal plane while rotating each magnetic mirror individually, we were able to correct the angle of incidence for small angular offsets. A mechanical chopper located upstream of the magnetic reflectometer produces a square wave modulation of the X-ray beam at 68 Hz with two practical advantages: (i) the heat load on the reflectometer is reduced by a factor of 2; (ii) the modulation signal can be fed into the reference input of a digital lock-in (VDL) (Gauthier *et al.*, 1995).

2.2. *Mechanical design of the reflectometer*

The 'white beam station' is equipped with a UHV-compatible stainless-steel chamber that can be rotated around the beam axis (Goulon *et al.*, 1996) and is mounted on a standard experimental table with remotely controlled horizontal and vertical translations (T_x, T_z). The small volume of the chamber required us to design a very compact reflectometer (Fig. 1). The two mirrors have independent mechanics and are mounted on two symmetric ports of the vacuum chamber. The CF100 flanges could be used as reference planes since they were carefully remachined after welding in order to be sure of the geometry of the chamber. Each mirror has two independent degrees of freedom: (i) a horizontal translation (T_{x1}, T_{x2}) perpendicular to the beam direction can be generated by a motorized translation table (Schneeberger AG) with a resolution of 2 μm; (ii) an accurate rotation of the mirror around its vertical symmetry axis ($\Delta\theta_{max} = \pm 30$ μrad) is produced by a flexure hinge actuated by a motorized micrometer screw (Physik-Instrumente) with a resolution better than 20 μrad. Since all motors and the two translation tables were kept outside the vacuum chamber, rods and UHV bellows were needed. Heidenhain MT12 sensors assess the reproducibility of the rotations.

A copper coil magnetizes a soft-iron circuit which encompasses the magnetic reflective layer of mirror M_2. The magnetization is parallel to the beam direction and it is possible to flip its orientation at *ca* 1 Hz (Fig. 1*a*). With a current of 2 A, a magnetic field of the order of 0.1 T was measured with a Hall probe. A cooling system is available in order to evacuate the heat load due to the absorption losses and to the power dissipated in the coil. Indeed, it is essential to keep the sample below its Curie temperature. A cryogenic system is available, which consists of a liquid-nitrogen-cooled copper block with flexible copper braids connected to the magnetic circuit and to the mirror support. Even though the cooling efficiency of this system is limited, we had no difficulty in keeping the temperature of the mirrors below 260 K while flipping the magnetic field at a frequency of 1 Hz.

2.3. *Magnetic mirrors*

Each mirror was made of a thick silicon wafer cut to the appropriate shape (L = 25 mm, W = 8 mm, T = 7 mm). The microroughness of the bare surface was 2 Å r.m.s. The first mirror, M_1, was coated with a cobalt layer (*ca* 1000 Å thick) and the second one, M_2, with a thin film of $Fe_{67}Rh_{33}$ magnetic alloy (also *ca* 1000 Å thick). Both mirrors were capped with a 20 Å thin aluminium layer in order to prevent any surface oxidation. Magneto-optical Kerr-effect measurements on mirror M_1 confirmed that saturation was reached with a magnetic field H_{sat} = 500 Oe with a coercive field H_{coerc} = 120 Oe.

2.4. *Normalization of reflectivity spectra*

A major difficulty arises from the lack of a suitable detector I_0^- to normalize the beam intensity fluctuations. Two different methods were considered to renormalize reflectivity spectra:

(*a*) At high grazing incidence (<8 mrad), it is possible to slightly mistune the parallelism of the double-mirror reflectometer in order to split the incident beam into (i) a reflected beam, plus (ii) a non-reflected (*i.e.* transmitted) beam, which reach the BPM at different positions. It then becomes possible to normalize the intensity of the reflected beam with respect to the total intensity. This improved the signal-to-noise ratio of our Refl-EXAFS spectra considerably.

(*b*) Unfortunately, the latter technique becomes impracticable for large angles of incidence as the transmitted beam is cut. For differential reflectivity experiments, it is most convenient to normalize the difference signal with respect to the sum, *i.e.* to measure directly a quantity proportional to the magnetic asymmetry ratio with a noise level of a few 10^{-4} in a single scan. Note that the polarization-averaged edge spectrum can be measured independently with another experimental configuration exploiting the monochromatic beam.

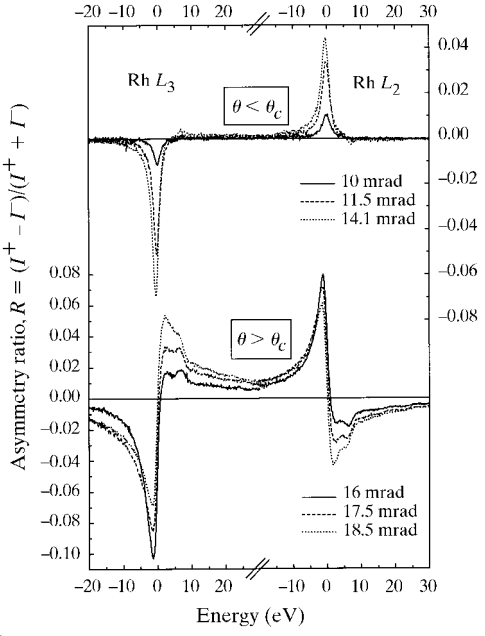

Figure 2
XMR spectra recorded at the rhodium $L_{2,3}$ edges for various incidences with either $\theta > \theta_c$ or $\theta < \theta_c$. Note the changes of the lineshapes.

3. Results

We have reproduced in Fig. 2 a series of differential X-ray magnetic reflectivity (XMR) spectra recorded at room temperature at the $L_{2,3}$ edges of rhodium for several angles of incidence. We kept the helicity of the X-ray photons fixed and reversed the direction of the magnetization four times for each data point of

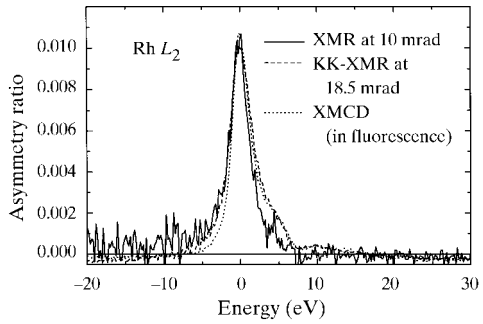

Figure 3
Comparative display of the Kramers–Kronig (KK) transform of the L_2-edge XMR spectrum recorded at 18.5 mrad grazing incidence, together with the L_2-edge XMR spectrum recorded at 10 mrad grazing incidence and the XMCD spectrum recorded on the same sample at the same edge using the conventional FY detection scheme. Note that all spectra can be satisfactorily superimposed as predicted by our analysis.

an energy scan. Fig. 2 shows the asymmetry ratio averaged over four consecutive scans. We checked that inverted spectra were obtained on switching the undulator to the opposite photon helicity. Note that the asymmetry ratio has the opposite sign at the L_2 and L_3 edges, in full agreement with the XMCD sum rules. As already noted by Kao *et al.* (1994), there are large changes in the intensity of the signal and in the measured lineshapes when the angle of incidence is modified. What adds considerable involvement to the analysis of magnetic reflectivity experiments is the fact that the reflectivity depends on both the real (δ) and the imaginary part (β) of the complex refractive index. For simplicity, one may first forget about the contribution of magnetic diffuse scattering by the surface and start with the Nevot–Croce model of reflectivity for a single optical interface that can be characterized by a small microroughness s (Nevot & Croce, 1980). It can be shown that, at the critical angle of incidence (θ_c), the asymmetry ratio induced by the magnetic ordering can be written as (Neumann *et al.*, 1998)

$$\Delta R/R = (\Delta R_F/R_F) + (\Delta D_{NC}/D_{NC}), \quad (1)$$

where R_F refers to the Fresnel reflectivity

$$\Delta R_F/R_F = [(2\bar{Y})^{1/2}/(1+\bar{Y}^2)]\{\eta_H[(1/\bar{Y})+2] - \zeta_H\} \quad (2)$$

and D_{NC} refers to the Nevot–Croce correction for rough surfaces,

$$\Delta D_{NC}/D_{NC} = (2\bar{Y})^{1/2} k_1^2 \sigma^2 \theta_c^2 [(\eta_H/\bar{Y}) - \zeta_H], \quad (3)$$

where $\bar{Y} = \bar{\beta}/\bar{\delta} \ll \delta = \bar{\delta}(1+\eta_H)$ and $\beta = \bar{\beta}(1+\zeta_H)$.

From equations (2) and (3) it can be seen that, at the critical angle of incidence, the XMR spectra are dominated by the dispersive part $\eta_H(E)$, even for rather rough surfaces. In other words, XMR spectra recorded at the critical angle of incidence should be more or less equivalent to Faraday rotation spectra (Siddons *et al.*, 1990; Kortright *et al.*, 1995). Some more involved calculations (Neumann *et al.*, 1998) would lead to the opposite conclusion when the angle of incidence is much smaller than the critical angle. To illustrate this prediction we have calculated the odd-parity Kramers–Kronig transform of the XMR spectrum recorded at 18.5 mrad, *i.e.* very near the expected critical angle (14.4 mrad): if our theory is correct, the Kramers–Kronig-transformed spectrum should reproduce the lineshape of an XMCD spectrum. This is precisely confirmed by Fig. 3, which also shows that the XMR spectrum recorded at 10 mrad incidence is unambiguously dominated by the XMCD lineshape.

4. Conclusions

High-quality differential XMR spectra have been recorded at the $L_{2,3}$ edges of rhodium. The most attractive advantage of our configuration is that it takes full benefit of the high polarization rate of the source. It is also shown that, by properly selecting the angle of incidence, one may obtain experimental X-MR spectra dominated either by dispersion or absorption terms. A natural extension of these experiments would concern the investigation of buried interfaces of magnetic multilayers: more information might be extracted from the Bragg diffraction peaks associated with the magnetic superlattice as pioneered by Tonnerre *et al.* (1995).

We are grateful to J.-F. Bouteille for his advice regarding the design of the magnetic circuit and to Yves Souche (CNRS, Grenoble) for magneto-optical Kerr-effect measurements. We are also indebted to Gerry Harp and his group from Ohio University for the preparation of the $Fe_{67}Rh_{33}$ magnetic alloy.

References

Baibich, M. N., Broto, J. M., Fert, A., Dau, N. V., Petroff, F., Etienne, P., Creuzet, G., Friederich, A. & Chazelas, J. (1988). *Phys. Rev. Lett.* **61**, 2472–2475.
Bisnasch, G., Grünberg, P., Saurenbach, F. & Zinn, W. (1989). *Phys. Rev. B*, **39**, 4828–4830.
Carra, P., Thole, B. T., Altarelli, M. & Wang, X. D. (1993). *Phys. Rev. Lett.* **70**, 694–697.
Elleaume, P. (1994). *J. Synchrotron Rad.* **1**, 19–26.
Gauthier, C., Goujon, G., Feite, S., Moguiline, E., Braicovich, L., Brookes, N. B. & Goulon, J. (1995). *Physica (Utrecht)*, B**208**/**209**, 232–234.
Goulon, J., Malgrange, C., Giles, C., Neumann, C., Rogalev, A., Moguiline, E., De Bergevin, F. & Vettier, C. (1996). *J. Synchrotron Rad.* **3**, 272–281.
Goulon, J., Rogalev, A., Gauthier, C., Goulon-Ginet, C., Paste, S., Signorato, R., Neumann, C., Varga, L. & Malgrange, C. (1998). *J. Synchrotron Rad.* **5**, 232–238.
Harp, G. R., Parkin, S. S. P., O'Brien, W. L. & Tonner, B. P. (1995). *Phys. Rev. B*, **51**, 12037–12040.
Kao, C.-C., Chen, C. T., Johnson, E. D., Hastings, J. B., Lin, H. J., Ho, G. H., Meigs, G., Brot, J.-M., Hulbert, S. L., Idzerda, Y. U. & Vettier, C. (1994). *Phys. Rev. B*, **50,** 9599–9602.
Kobayashi, K., Maruyama, H., Iwazumi, T., Kawamura, N. & Yamazaki, H. (1996). *Solid State Commun.* **97**, 491–496.
Kortright, J. B., Rice, M. & Carr, R. (1995). *Phys. Rev. B*, **51**, 10240–10243.
Lambrecht, W. R. L., Rashkeev, S. N., Segall, B., Lawniczak-Jablonska, K., Suski, T., Gullikson, E. M., Underwood, J. H., Perera, R. C. C., Rife, J. C., Grzegori, I., Porowski, S. & Wickenden, D. K. (1997). *Phys. Rev. B*, **55**, 2612–2622.
Malgrange, C., Carvalho, C., Braicovich, L. & Goulon, J. (1991). *Nucl. Instrum. Methods A*, **308**, 390–396.
Neumann, C., Rogalev, A. & Goulon, J. (1998). In preparation.
Nevot, L. & Croce, P. (1980). *Rev. Appl. Phys.* **15**, 761–769.
Siddons, D. P., Hart, M., Amemiya, Y. & Hastings, J. B. (1990). *Phys. Rev. Lett.* **64**, 1967–1970.
Stöhr, J. & Nakajima, R. (1997). *J. Phys. (Paris) (C2)*, **7**, 47–57.
Thole, B. T., Carra, P., Sette, F. & van der Laan, G. (1992). *Phys. Rev. Lett.* **68**, 1943–1946.
Tonnerre, J. M., Sève, L., Raoux, D., Soullié, G., Rodmacq, B. & Wolfers, P. (1995). *Phys. Rev. Lett.* **75**, 740–743.
Vogel, J., Fontaine, A., Gros, V., Petroff, F., Kappler, J.-P. & Krill, G. (1997). *Phys. Rev. B*, **55**, 3663–3669.